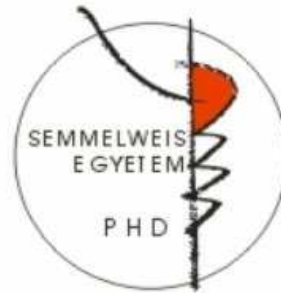# FDG PET investigation in malignant diseases, with a special focus on its prognostic role in lymphomas

PhD thesis

Tamás Györke MD

Semmelweis University
Doctoral School of Clinical Medical Sciences

Supervisor: Tamás Masszi MD, Ph.D.

Official reviewers: Katalin Zámbó MD, Ph.D
Zsuzsanna Orosz MD, Ph.D

Head of the Final Examination Committee:
Dániel Bereczki MD, D.Sc

Members of the Final Examination Committee:
László Galuska MD, Ph.D
Judit Müller MD, Ph.D

Budapest

2012

1. INTRODUCTION

Positron Emission Tomography (PET) or PET combined with Computed Tomography (PET-CT) using ^{18}F-Fluoro-Deoxi-Glucose (FDG) is a fundamental diagnostic investigation in several oncological diseases.

In the thesis I discuss my scientific results obtained with FDG PET and PET-CT in two types of tumours, the Ewing sarcoma family tumours and the lymphomas.

The heterogeneous group of bone and soft tissue sarcomas includes several tumour entities with a low prevalence, accordingly the body of evidence about the impact of PET is also limited.

FDG PET is a standard diagnostic procedure in the staging and post treatment restaging of Hodgkin lymphomas (HL) and aggressive non-Hodgkin lymphomas. There are also promising data concerning the interim PET (iPET) evaluating early therapy response which may help the more effective application of personalized treatment based on a response adapted approach.

Specifically in diffuse large B-cell lymphomas (DLBCL) there are controversial results regarding the predictive value of iPET which are partially correlated with the fact that interpretation criteria of iPET are not standardised. In a consensus meeting in 2009 in Deauville (France) a 5-point scale scoring system was recommended as the standard way of visual evaluation (Deauville criteria = DC). A French group (Lin et al. J Nucl Med, 2007) reported the superiority of a semiquantitative SUV-based (SUV=Standardized Uptake Value) interpretation over visual one. For both methods validation studies were encouraged in independent groups of subjects.

In case of positive iPET findings histological clarification may be required in order to define further therapy. However, non-palpable lesions can make difficult the surgical localisation during biopsy. The radioguided occult lesion localisation (ROLL) technique has been developed and routinely used for the preoperative labelling of non palpable occult breast lesions requiring diagnostic or therapeutic excision.

2. AIMS

2.1. Diagnostic impact of FDG-PET of Ewing sarcomas and primitive neuroectodermal tumours

Our purpose was to evaluate retrospectively the value of ^{18}FDG-PET in a relatively homogenous group of tumours of the Ewing family (ET) which is made up by Ewing Sarcomas (ES) and Primitive Neuroectodermal Tumours (PNET). .

3.2. The prognostic role of iPET in DLBCL performed after two cycles of immunochemotherapy: comparison of visual and semiquantitative evaluation

The aim of this study was the comparison of DC-based visual and SUV-based semiquantitative evaluation and defining the predictive value of iPET in a large, homogenous patient cohort.

3.3. Radioguided lymph node biopsy of a chemoresistant lymph node detected on interim FDG PET-CT in Hodgkin lymphoma

We report the adaptation and successful application of ROLL for guiding the surgical biopsy of a chemoresistant lymph node detected by interim FDG PET-CT.

3. METHODS

3.1. Diagnostic impact of FDG-PET of Ewing sarcomas and primitive neuroectodermal tumours

3.1.1. Patients

We included in this retrospective study 33 FDG-PET examinations performed on 24 patients (17 males, 7 females; ages: 6-62, mean: 28.4 years) with a suspected or histologically confirmed ET between January 1996 and June 2002 at the Albert-Ludwigs University in Freiburg (Germany).

One investigation was performed in 17, two in 6 and four in 1 patient. The histological diagnoses of primaries were as follows: 10 ES of the bone, 13 PNET (6 soft

tissue, 7 bone lesions) and 1 osteomyelitis. 16 examinations were performed at the first presentation with the primary lesion and 17 later on during the course of the disease.

The findings of 14 PET examinations in 14 patients were compared with whole-body bone scintigraphy (BS) performed 1-21 days (mean: 8.3 ± 7.9) before or after PET.

3.1.2. Imaging methods

After the patients had fasted for 12 h, 5 MBq FDG per kilogram of body weight were injected into a peripheral vein. Static 2D whole-body PET was performed with a Siemens ECAT-EXACT 922 tomograph beginning 90 min after tracer injection. An emission image and a transmission image (using an external germanium source) were recorded. Coronal, sagittal, and transaxial images were produced on the basis of an iterative reconstruction algorithm using ordered-subset expectation maximization and segmented attenuation correction after injection.

BS was performed 3 hours after the intravenous administration of ^{99m}Tc-DPD using a whole-body gamma camera (Siemens Bodyscan).The administered dose was about 700 MBq for adults and calculated for children according to the recommendations of the European Association of Nuclear Medicine.

3.1.3. Image analysis

The PET images were interpreted blindly to the results of other imaging studies and independently by two experienced investigators. The physicians interpreted any focally-increased radiotracer uptake that exceeded the normal limits of regional FDG accumulation in the area as either benign or malignant. The maximal SUV (SUV_{max}) was calculated for semiquantitative evaluation of increased uptakes. SUV was compared with lesion size, when the exact size of a lesion at the time of PET investigation was known and available from morphological imaging (n=33). Bone scans were analysed visually.

3.1.4. Reference methods

The nature of findings in PET and/or other imaging methods was confirmed by histopathological analysis (in 22 lesions), results of imaging methods i.e. plain radiography, ultrasonography (US), CT, magnetic resonance imaging (MRI) and in all

but four cases a follow-up of at least 6 months (7-39, mean: 20.8±10.1 months). Four patients died after 15 – 120 days.

3.1.5. Statistical methods

Diagnostic sensitivity, specificity and accuracy were calculated both on lesion-based analysis and on examination-based analysis. The 95 % confidence interval (CI) for each parameter is given. The statistical significance was calculated using the Mann-Whitney test and a p-value of less than 0.05 was considered significant.

3.2. The prognostic role of iPET in DLBCL performed after two cycles of immunochemotherapy: comparison of visual and semiquantitative evaluation

3.2.1. Patients

The International Atomic Energy Agency (IAEA) is coordinating and sponsoring a prospective international multicentre cohort study which inclusion and exclusion criteria are listed in *Table 1*. We used the data of 293 patients enrolled between 1. January 2007. and 30. June 2011. in six participating countries (Brazil, Chile, Hungary, Italy, Philippines, and Thailand).

Table 1. Inclusion criteria for the IAEA study

Inclusion criteria	Exclusion criteria
Newly diagnosed DLBCL or PMBCL	Primary central nervous system lymphoma
Age above 15years	Primary bone lymphoma
Able to comply with study treatment, monitoring and follow up protocol	Stage I. with negative pre-treatment PET scan
Informed consent obtained	Diabetes mellitus requiring medication
	Mental incapacity
	Malignancy in history within 5 years
	Severe comorbid diseases
Abbreviations: DLBCL: diffuse large B-cell lymphoma, PMBCL: primary mediastinal large B-cell lymphoma,	

According to the IAEA study protocol the first line treatment consisted of CHOP (cyclophosphamide, doxorubicine, vincristine, prednisone) or CHOP-like chemotherapy with or without rituximab. Patients were investigated by means of PET or PET-CT within one month before the start of treatment (PET-0), after 2 or 3 treatment cycles (iPET) and following the first line therapy (PET-post).

We included subjects into our study if: *a)* treatment contained rituximab, *b)* PET-0 and iPET were performed with the same camera and the same reconstruction

parameters, *c)* anonymized full PET-0 and iPET were available in DICOM (Digital Imaging and Communications in Medicine) format at the Research Coordination Meeting held in March 2012. *d)* iPET was performed after 2 cycles of immunochemotherapy (PET-2), *e)* follow-up at closure of database was at least 24 months from the start of treatment, if treatment failure (TF) hasn't occurred.

Based on the above criteria 113 patients were included (Brazil: 44, Chile: 21, Hungary: 33, Italy: 0, Philippines: 3, Thailand: 12).

The IAEA study was approved by the respective ethical review board of each country.

The patient characteristics are summarized in *Table 2*.

Table 2. Patient characteristics

Characteristic	n=113	Characteristic (continued)	n=113
Age: median (range)	55 (16-84) years	*aaIPI risk*	
Sex: male/female	54/59 (48/52%)	low	27 (24%)
Histological subtype		low-intermediate	37 (33%)
DLBCL	108 (96%)	high-intermediate	35 (31%)
PMBCL	5 (4%)	high	14 (12%)
Stage		*prognosis according to R-IPI*	
I.	10 (9%)	very good (IPI: 0)	17 (15%)
II.	33 (29%)	good (IPI: 1-2)	59 (52%)
III.	24 (21%)	poor (IPI: 3-5)	37 (33%)
IV.	46 (41%)	*Immunochemotherapy*	
Performance state: ECOG ≥2	18 (16%)	R-CHOP-21 4-8 cycles**	95 (84%)
Number of extranodal manifestations ≥2	30 (27%)	R-CHOP-14 4-8 cycles**	15 (13%)
Elevated LDH level	61 (54%)	R-CEOP-21 4-8 cycles**	3 (3%)
Bulky tumour		*Consolidation IFRT*	41 (36%)
bulky*	35 (31%)		
very extensive disease*	29 (26%)		

DLBCL: diffuse large B-cell lymphoma, PMBCL: primary mediastinal large B-cell lymphoma, ECOG: Eastern Cooperative Oncology Group, LDH: lactate-dehydrogenase, IPI: international prognostic index, aaIPI: age adjusted IPI, R-IPI: revised IPI, R-CHOP-21: rituximab, cyclophosphamide, doxorubicine, vincristine, prednisolone in 3 weeks interval, R-CHOP-14: R-CHOP in 2 weeks interval, R-CEOP-21: like R-CHOP-21, epirubicine instead doxorubicin, IFRT: involved field radiation therapy
*bulky tumour: diameter >5 cm, very extensive disease: >10 cm or at least two lesions with diameter> 7 cm
**planned number of cycles was defined according to local preferences: in stage I-II. minimally 4 cycles, in stage III-IV. 6-8 cycles

3.2.3. FDG PET and PET-CT investigations

FDG PET investigations were performed by dedicated PET or PET-CT cameras (PET: Brazil, PET-CT: Chile, Hungary, Philippines and Thailand). Following 6 hours of fasting state and the injection of 6,4 ± 1,5 MBq/kg (mean) of FDG whole body PET was made after a median uptake time of 69 minutes (range: 40-187 minutes). Images with and without attenuation correction were produced. The result of PET-2 was not allowed

to influence the planned therapy, unless PET-2 showed a proven progression.

3.2.4. The evaluation methods of PET investigations

I performed the evaluation of PET images with Interview Fusion software (Mediso Ltd., Budapest), blinded to disease outcome. Positive iPET scan was defined as a scan with focal area of increased FDG uptake compared to local background not attributable to physiological or other benign causes.

3.2.4.1. Visual interpretation of iPET based on the Deauville criteria

Pathological uptakes were compared to mediastinal blood pool (MBP) and liver activity and scored on a 5-point scale according to Deauville criteria (DC) *(Table 3.)*.

Table 3. The Deauville criteria

Score	Pathological FDG uptake
1	No uptake
2	Uptake equal or less than MBP
3	Uptake more than MBP but equal or less than liver activity
4	Uptake moderately increased compared with the liver at any site
5	Uptake markedly increased compared with the liver at any site or/and new sites of disease
MBP: mediastinal blood pool, Proposal: Scores 4-5 should be regarded as positive	

3.2.4.2. Semiquantitative evaluation

SUVmax was defined by VOI (Volume of Interest) technique in pathological uptakes. The SUV was measured according to the most intense FDG uptake on PET-0 (SUV-$0_{max-max}$) and on PET-2 (SUV-2_{max}). On PET-0 SUV was defined for that lesion too which corresponded in localisation to the hottest lesion on PET-2 (SUV-$0_{max-int}$). On PET-2 images I measured the maximal (SUV-máj$_{max}$) and mean (SUV-máj$_{átl}$) SUVs of the liver using a VOI placed into the right lobe of the liver.

The SUV change between PET-0 and PET-2 investigations was characterised by the percentage ΔSUV: ΔSUV$_{max}$= (1-(SUV-2_{max} / SUV-0_{max}))*100. ΔSUV was calculated both for SUV-$0_{max-max}$ and SUV-$0_{max-int}$ (ΔSUV$_{max}$ and ΔSUV$_{int}$).

The percentage ratio of SUV-2_{max} compared to liver activity was also defined: SUV-2/máj$_{max}$ = (SUV-2_{max} / SUV-máj$_{max}$)*100.

3.2.5. Post treatment disease status and follow-up

The post treatment disease status was determined by PET-CT or PET and CT

investigations performed after the end of first line therapy and evaluated according to the revised Cheson criteria. Following this patients were clinically checked regularly. The database containing the follow-up data was closed on 30. March 2012. for this study.

3.2.6. Statistical analysis

To evaluate the early prognostic value of iPET, 2 year event-free survival (EFS) was chosen as endpoint. EFS was defined as the interval from the start of treatment to the first evidence of a TF (primary treatment resistance, progression, relapse or death of the patient). Data of patients without TF were censored at last follow-up.

Continuous variables were compared using the Independent-Samples T-test or Mann-Whitney test if variables were not normally distributed.

Receiver operating characteristic (ROC) analysis was performed to compare the diagnostic accuracy of several evaluation methods and to determine an optimal cut-off for the different parameters predicting treatment failure, i.e. a threshold for iPET positivity.

Estimates of survival were calculated according to the Kaplan-Meier method and compared with the log-rank test. Significance was obtained when the p value was less than 0.05.

3.3. Radioguided lymph node biopsy of a chemoresistant lymph node detected on interim FDG PET-CT in Hodgkin lymphoma

A 32-year-old male patient was diagnosed with nodular lymphocyte-predominant Hodgkin lymphoma. Staging FDG PET-CT detected a large right axillary lymph node conglomerate and splenic manifestation, indicating stage III disease. ABVD (adriamycin, bleomycin, vinblastine and dacarbazine) chemotherapy was started. After the 2nd and 4th cycles of chemotherapy interim PET-CT investigations were performed, revealing good metabolic response both in the right axilla and the spleen with the exception of a single enlarged right axillary lymph node which showed only moderate decrease of FDG uptake compared with the staging investigation. Histological examination was required for the clarification of the persistently high uptake. However, the metabolically active lymph node was non-palpable and several

other residual similarly enlarged lymph nodes were present without metabolic activity. The ROLL technique was used for guiding the biopsy. Based on an US examination of the right axillary region with a thorough side by side comparison to the PET-CT images, the metabolically active lymph node could also be identified by US. For the ROLL procedure the radiopharmaceutical (0,15 ml of 15 MBq ^{99m}Tc labelled macroaggregate albumin) was injected under US guidance into the lymph node.

4. RESULTS

4.1. Diagnostic impact of FDG-PET of Ewing sarcomas and primitive neuroectodermal tumours

4.1.1. The diagnostic sensitivity and specificity of PET

PET investigations and/or reference methods revealed 163 evaluable lesions.

113 were categorized as true positives: 16 primaries, 5 residual or recurrent lesions, 68 bone metastases, 13 pulmonary or pleural metastases (size: 8-30 mm), 4 liver metastases (size: 13-15 mm) and 7 additional soft tissue metastases. The smallest true positive lesion (among lesions with known size) was an 8 mm large lung metastasis.

In 4 cases, MR investigation detected a lesion suspicious of recurrent disease and PET classified these lesions as true negatives. 3 further PET examinations showed no pathological uptake at all, considered to be also true negatives based on follow-up results.

2 false positive lesions were depicted in two patients: one osteomyelitis and in another patient a faintly increased uptake in the region of primary tumour without residual disease on follow-up.

In 7 patients, 41 metastatic or recurrent lesions were undetectable for PET: 32 pulmonary metastases (smaller than 1 cm), 6 liver metastases (under 1.3 cm in size), 1 bone metastasis (5 mm large) and following chemotherapy in one patient, 2 foci of recurrent ES with a diameter of 3 cm each.

The sensitivity, specificity and accuracy characterising the diagnostic value of PET on a lesion-based and on an examination based analysis are shown in *Table 4*.

4.1.2. Results of semiquantitative evaluation

The standard uptake values of true positive lesions were between 1.15 and 18.07 with a mean value of 4.54±2.79. The SUVs of lesions with a known size of 15 mm, or smaller (n=13) were between 1.15 and 4.25, mean 2.65±1.12, for lesions larger than 15 mm (n=20) between 2.46 and 18.07, mean 7.36±4.87. The difference between the SUVs of these smaller and larger sized lesions was significant (p=0.000081). Concerning the two false-positive lesions, SUV was 4.66 for osteomyelitis and 1.60 for the other indeterminate lesion.

Table 4. The diagnostic value of PET

	Sensitivity 95% CI	Specificity 95% CI	Accuracy 95% CI
Lesion-based analysis (n=163)	0,73 0,67-0,80	0,78 0,71-0,84	0,74 0,66-0,80
Examination-based analysis (n=33)	0,96 0,89-1,00	0,78 0,64-0,91	0,91 0,76-0,98

4.1.3. Comparison of PET and bone scintigraphy

The available 14 BSs detected all 11 primary bone lesions present at the time of investigation, but only 8 of 70 bone metastases, revealed by PET and MRI. 62 metastases of four patients remained undetected by BS.

4.2. The prognostic role of iPET in DLBCL performed after two cycles of immunochemotherapy: comparison of visual and semiquantitative evaluation

4.2.1. Disease outcome

The median follow-up was 27.2 months (range: 2-42 months) for all patients and 29.6 months (range: 24-42 months) for patients without TF. The results of disease outcome are illustrated on a flow chart *(Figure 1.)*.

4.2.2. The distribution of iPET results according to Deauville criteria

The distribution of iPET results according to DC is summarized in *Table 5*.

4.2.3. The Standardized Uptake Values (SUV)

There was no statistically significant difference between SUV-$0_{max-max}$ of patients with TF and event-free subjects. In contrast, for SUV-2_{max}, ΔSUV and
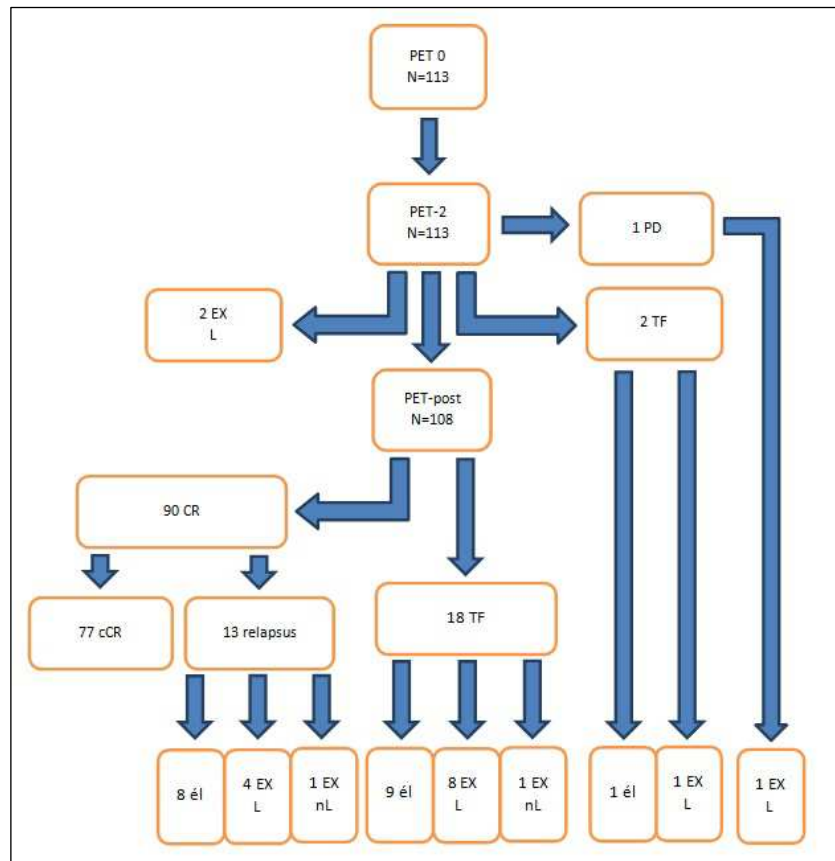
Figure 1. Flow chart of disease outcome. PD: progression, TF: treatment failure, CR: complete remission, cCR: continous CR, EX: death, L: lymphoma related, nL: not L, él: alive

Table 5. Distribution of iPET results according to Deauville criteria

DC score	Number of patients	Number of patients with TF	Number of patients without TF
1 (no increased uptake)	21 (18.6%)	0	21
2 (>BG, but ≤MBP)	19 (16.8%)	2	17
3 (>MBP, but ≤LIVER)	25 (22.1%)	3	22
4 (moderately >LIVER)	27 (23.9%)	13	14
5 (markedly >LIVER and/or new lesion)	21 (18.6%)	18	3
Sum	*113 (100%)*	*36 (32%)*	*77 (68%)*

DC: Deauville criteria, TF: treatment failure, BG: background, MBP: mediastinal blood pool

SUV-2/máj$_{max}$ values the difference was statistically significant. The mean and median values of the several parameters in the two patient groups are shown tabulated *(Table 6.)*.

Table 6. SUV-based parameters in patient groups with or without treatment failure

parameter	with TF		without TF		significance
	mean	*median*	*mean*	*median*	
SUV-$0_{max-max}$	22.2 ± 12.2	20.9 (5.3-55.6)	22.8 ± 11.9	20.6 (4.6-50.4)	p =0.735
SUV-2_{max}	7.4 ± 5.6	5.3 (1.8-29.4)	3.1 ± 2.5	2.6 (0.9-19.6)	p <0.00001
ΔSUV_{max}	57.9 ± 33.3	69.7 (-31.6-93.7)	84.4 ± 8.9	86.4 (50.1-96.8)	p <0.00001
ΔSUV_{int}	46.1 ± 47.2	62.7 (-111.4-93.7)	81.8 ± 10.6	84.2 (50.1-96.8)	p <0.00001
SUV-2/máj$_{max}$	227.1 ± 163.2	175 (74.6-789.8)	92 ± 75.8	73 (24.4-533.2)	p <0.00001

TF: treatment failure

4.2.4. ROC analysis

The area under the ROC curve (AUC) was not significant in case of SUV-$0_{max-max}$ (AUC =0.52, p =0.732). The other five methods proved to be similarly accurate and with the comparison of each AUC no statistically significant difference was obtained. Using ROC analysis the optimal cut-off value of each parameter was determined. These and the corresponding sensitivity and specificity values are summarized in the following table (*Table 7.*). 48.9% cut-off of ΔSUV_{max} represented 100% specificity.

Table 7. Results of ROC analysis of the evaluation parameters

parameter	AUC	significance	optimal cutoff		
			value	*sensitivity (%)*	*specificity (%)*
SUV-$0_{max-max}$	0.52	p =0.7323	–	–	–
DK score	0.88	p <0.0001	3.5	86.1	77.9
SUV-2_{max}	0.84	p <0.0001	4.3	77.8	84.4
ΔSUV_{max}	0.80	p <0.0001	78.0%	72.2	81.8
ΔSUV_{int}	0.82	p <0.0001	76.9%	83.3	74.0
SUV-2/máj$_{max}$	0.87	p <0.0001	113%	80.6	80.5

AUC: area under the curve

4.2.5. Kaplan-Meier analysis

4.2.5.1. Predictive values of visual interpretation

The comparison of EFS probability between iPET-negative (iPET−) and iPET-positive (iPET+) groups were performed using two criteria for iPET postivity: *1)* iPET is positive if the score according to DC is 3, 4 or 5; *2)* iPET is positive if the score is 4

or 5. Results of both criteria are listed in *Table 8*. The second approach had unequivocally better results than the first one, however the positive predictive value (PPV) of 64.6% is rather low, while the negative predictive value (NPV) of 92.3% is excellent.

Table 8. Results of iPET interpretation using different criteria

iPET positive, if	Sensitivity (%)	Specificity (%)	NPV (%)	PPV (%)	Accuracy (%)	iPET− 2y EFS (%)	iPET+ 2y EFS (%)	p value (log-rank)
Visual interpretation								
DC =3, 4, 5	94,4	49,4	95,0	46,6	63,7	95	55	<0,001
DC = 4, 5	86,1	77,9	92,3	64,6	80,5	92	37	<0,001
Semiquantitative interpr.								
ΔSUV_{max} <78%	72,2	80,5	86,1	63,4	77,9	86	39	<0,001
ΔSUV_{max} <66%	44,4	94,8	78,5	80,0	78,8	79	25	<0,001
**ΔSUV_{max} <49%	27,8	100	74,8	100	77	76	0	<0,001
ΔSUV_{int} <76,9%	83,3	74,0	90,5	60,0	77,0	91	42	<0,001
SUV-2/máj$_{max}$ >113%	80,6	80,5	89,9	65,9	80,5	90	36	<0,001
SUV-2/máj$_{max}$ >140%	66,7	87,0	84,8	70,6	80,5	85	32	<0,001
SUV-2$_{max}$ >4,3	77,8	84,4	89,0	70,0	82,3	89	33	<0,001
***Combined interpr.*								
DK =4, 5 and ΔSUV_{max} <66% (n=81, 72%)	78,9	95,2	93,7	83,3	91,4	94	22	<0,001
DK =4, 5 and ΔSUV_{max} <49% (n=75, 66%)	66,7	100	92,3	100	93,3	92	0	<0,001

Abbreviations: iPET: interim PET, NPV: negative predictive value, PPV: positive predictive value, 2y EFS: 2 year event-free survival, DC: Deauville criteria

** ΔSUV_{max} =49%: cut-off point for 100% specificity based on ROC analysis

*** iPET is positive, if both visually (DK =4-5) and quantitatively positive; iPET is negative if negative with both methods

4.2.5.2. Predictive values of semiquantitative evaluation

Semiquantitative evaluation was performed using both the optimal cut-off values obtained by ROC analysis and threshold parameters reported by other authors, i.e. ΔSUV_{max} =66% and SUV-2/máj$_{max}$ =140% *(Table 8.)*.

The application of cut-off values calculated by own ROC analysis didn't perform reasonably better than visual interpretation (iPET+ if DK =4-5). In contrast, using the 66% ΔSUV_{max} threshold resulted in a PPV of 80%.

4.2.5.3. Predictive values of combined evaluation

The visual (iPET+ if DC =4-5) and semiquantitative (iPET+ if ΔSUV_{max} <66%) evaluations had concordantly negative or positive results in case of 81 patients (71.7% of all patients). Creating an „unequivocally" iPET+ and an „unequivocally" iPET− group according to these cases, an outstanding PPV of 83% and NPV of 94% could

have been reached in the same time among 72% of all patients. Applying the same approach with the 48.9% ΔSUV_{max} value as the semiquantitative threshold for iPET positivity in case of 66.3% of all patients the PPV and NPV could have been 100% and 92%, respectively *(Table 8.)*.

4.3. Radioguided lymph node biopsy of a chemoresistant lymph node detected on interim FDG PET-CT in Hodgkin lymphoma

The lymph node was successfully removed by a minimally invasive procedure with local anaesthesia using a hand held surgical gamma probe. Histological evaluation of the node revealed a T cell-rich diffuse large B-cell lymphoma.

Based on this finding, a more aggressive therapeutic approach was required. Accordingly, the patient was given two cycles of R-DHAP (rituximab, dexamethasone, high-dose Ara-C, cis-platine). Peripheral blood stem cells were collected after the first cycle. Autologous stem cell transplantation was subsequently performed with a BEAM (carmustine, etoposide, cytarabine, and melphalan) conditioning regimen. The patient was in complete remission 2.5 years after the transplantation.

5. CONCLUSIONS

5.1. Diagnostic impact of FDG-PET of Ewing sarcomas and primitive neuroectodermal tumours

The results and figures of diagnostic accuracy of PET in ETs are generally encouraging. The inherent advantage of PET is the simultaneous investigation of soft tissues and bones and the capability for whole body investigation. PET is very sensitive in the detection of both primary and recurrent lesions.

In agreement with the literature, there is lower sensitivity for small lesions, which causes a disadvantage particularly in the screening for lung metastases, so spiral CT takes obvious priority in this regard. However, using PET-CT equipment there is the possibility for the clarification of lung metastases during one single examination.

PET remarkably exceeds whole-body bone scintigraphy in ability to detect bone metastases, while with a limited field of view, routine MRI was also very effective for this purpose.

PET is unable to help in the noninvasive differentiation between the radiologically frequently indistinguishable ES and osteomyelitis.

SUV can help in lesion characterisation but in small lesions SUV may be decreased due to technical reasons. SUV or other quantitative parameters may be essential in assessing therapy response by PET.

In our patient population PET proved to be very useful in ruling out noninvasively viable tumour cells in suspected mass lesions and provided a higher degree of diagnostic safety, nevertheless it didn't lead to dramatic changes in patient management.

In conclusion, FDG-PET investigation can be recommended whenever it is available, but the determination of its exact role and place in the diagnostic workup of ETs needs further prospective investigation, due to its low incidence preferably in the frame of multicentre studies which are able to recruit higher number of subjects.

5.2. The prognostic role of iPET in DLBCL performed after two cycles of immunochemotherapy: comparison of visual and semiquantitative evaluation

Interim PET performed after 2 cycles of immunotherapy in this large homogenous series of DLBCL patients had good prognostic value interpreted either visually or semiquantitatively.

In contrast to previous reports, the maximal SUV measured on pre-treatment PET scans doesn't have any predictive value.

Our study confirms in the largest patient cohort so far the effectivity of Deauville criteria proposed for visual interpretation of iPET if residual uptakes higher than liver activity (i.e. DC =4-5) are regarded as positive.

This study is the first to confirm objectively using ROC analysis that in case of DLBCL iPET performed after 2 cycles of immunochemotherapy should be regarded as positive if residual uptake higher than liver activity is present, in agreement with the recommendation of DC.

We have determined by ROC analysis different cut-off values for semiquantitative parameters compared to literature data (ΔSUV_{max}: 78 vs. 66%, SUV-2/máj$_{max}$: 113 vs. 140%, SUV-2$_{max}$: 4.3 vs. 5). Using these thresholds the predictive value of iPET couldn't be improved significantly in comparison to visual interpretation based on DC. This is an indirect proof for the superiority of DC over previous visual interpretation criteria.

Our study validated in the largest independent series of patients so far the ability of 66% ΔSUV_{max} cut-off reported previously to decrease the false positive rate of iPET results compared to visual analysis.

Among the semiquantitative positivity criteria determined by other authors in different patient populations the ΔSUV_{max}-based parameter proved its superiority over the SUV-2/máj$_{max}$-based one, in agreement with respective literature data.

Compared to the international literature this is the first study which determined the ΔSUV_{max} cut-off value of 49% resulting in 100% specificity of iPET.

With the combination of visual and semiquantitative evaluation (iPET is positive if DC =4-5 and ΔSUV_{max} <66 or 49%) a new interpretation system was elaborated. Although a third group with equivocal prognostic significance has appeared beside the iPET+ and iPET− groups, in the two third of our patients the positive and negative predictive value of iPET could have been reasonably high in the same time.

The effectiveness of the 49% ΔSUV_{max} cut-off and the combined evaluation should be validated in independent series of patients. If the validity of these methods was confirmed their application would cause a substantial improvement in DLBCL in the more reliable decisions on metabolic response based treatment modifications.

5.3. Radioguided lymph node biopsy of a chemoresistant lymph node detected on interim FDG PET-CT in Hodgkin lymphoma

The ROLL technique is an appropriate method in HL for the biopsy of chemoresistant non-palpable lymph nodes suspected by interim PET-CT.

The anatomic information given by the CT part of the combined PET-CT method has great relevance for a multimodality approach i.e. ultrasound guidance during ROLL procedure.

According to several recommendations, at present, for early therapy monitoring and risk stratification, midtreatment PET is best obtained in the context of a clinical trial. We have found the interim PET investigation to be useful also in routine clinical practice, because of the possibility of early detection of ineffective therapy or progressive disease. However, when a modification of therapy is considered on the basis of iPET results in the nonprotocol setting a biopsy is also recommended to prove progression or to rule out unrelated benign pathology or neoplasm or disease transformation. This situation arises in patients with dissociated response (like in our case) or appearance of FDG uptake in previously nonavid site.

6. LIST OF PUBLICATIONS

6.1. Publications related to the thesis

1. <u>Györke T</u>, Zajic T, Lange A, Schafer O, Moser E, Makó E, Brink I. (2006) Impact of FDG PET for staging of Ewing sarcomas and primitive neuroectodermal tumours. Nucl Med Commun, 27: 17-24.
   IF: 1.283

2. <u>Györke T</u>. (2006) Positron emission tomography in oncology: commentary. (Hungarian) Orvtovábbk Szle, 13: 54-57.

3. <u>Györke T</u>. (2008) Imaging methods in internal medicine: PET-CT. (Hungarian) Magy Belorv Arch, 61 Klnsz: 109-114.

4. <u>Györke T</u>. (2010) Hybrid technics: PET-CT, SPECT-CT. (Hungarian) Orvosképzés, 85 Klnsz.1: 16-17.

5. <u>Györke T</u>, Kollár A, Bottlik Gy, Szepesi Á, Bodó I, Masszi T, Bérczi V, Garai I. (2011) Radioguided lymph node biopsy of a chemoresistant lymph node detected on interim FDG PET-CT in Hodgkin lymphoma. Int J Hematol, 93: 545-550.
   IF: 1.268

6.2. Publications not related to the thesis

1. <u>Györke T</u>, Karlinger K, Galgóczy H. (1997) MR diagnosis of endometriosis − Review of the literature in connection with one case. (Hungarian) Magy Radiol, 71: 157-160.

2. Mester Á, Makó E, Ortutay J, Dévai T, Márton E, Györke T. (1997) Sacroiliac joint HRCT morphology in inflammatory diseases. (Hungarian) Osteol Közl, 5: 18-23.

3. Mester Á, Makó E, Kiss K, Györke T, Dévai T, Márton E. (1997) HRCT morphology of inflammatory changes of apophyseal facet joints. (Hungarian) Osteol Közl, 5: 122-127.

4. Mester Á, Makó E, Nagylucskay S, Karlinger K, Márton E, Györke T. (1999) High resolution computed tomography detection of alimentary factors related to arthropathies in inflammatory bowel diseases. Acta Aliment, 28: 171-181.
IF: 0.177

5. Györke T, Duffek L, Bártfai K, Makó E K, Karlinger K, Mester A, Tarján Z. (2000) The role of nuclear medicine in inflammatory bowel disease. A review with experiences of aspecific bowel activity using immunoscintigraphy with ^{99m}Tc anti-granulocyte antibodies. Eur J Radiol, 35: 183-192.
IF: 0.822

6. Karlinger K, Györke T, Makó E, Mester Á, Tarján Z. (2000) The epidemiology and the pathogenesis of inflammatory bowel disease. Eur J Radiol, 35: 154-167.
IF: 0.822

7. Mester ÁR, Makó EK, Karlinger K, Györke T, Tarján Z, Márton E, Kiss K. (2000) Enteropathic arthritis in the sacroiliac joint. Imaging and differential diagnosis. Eur J Radiol, 35: 199-208.
IF: 0.822

8. Tarján Z, Zágoni T, Györke T, Mester Á, Karlinger K, Makó EK. (2000) Spiral CT colonography in inflammatory bowel disease. Eur J Radiol, 35: 193-198.
IF: 0.822

9. Tarján Z, Tóth G, Györke T, Mester Á, Karlinger K, Makó EK. (2000) Ultrasound in Crohn's disease of the small bowel. Eur J Radiol, 35: 176-182.
IF: 0.822

10. Györke T, Bártfai K, Kopcsányi Zs, Kiss K, Kári B, Mester Á, Karlinger K, Makó E. (2001) The role of bone SPECT in the patients with malignancy. (Hungarian) Osteol Közl, 9: 223-227.

11. Karlinger K, Györke T, Makó E, Mester Á, Tarján Zs. (2001) The epidemiology and the pathogenesis of inflammatory bowel disease. (Hungarian) Lege Artis Med, 11: 644-645.

12. Forgács B, Mester Á, Györke T, Makó E. (2003) An experimental model for the ROC analysis of the diagnostic accuracy of conventional and digital skeletal radiology. (Hungarian) Osteol Közl, 11: 83-86.

13. Kis É, Nyitrai A, Várkonyi I, Bártfai K, Györke T, Máttyus I, Verebély T. (2003) Follow-up of infants undergoing pyeloplasty: renal ultrasound and diuresis renography changes. (Hungarian) Magy Radiol, 77: 170-174.

14. Kiss K, Szentmártoni Gy, Mester Á, Györke T, Makó E. (2003) A rare case of monostotic Paget's disease: ivory vertebra. (Hungarian) Osteol Közl, 11: 93-95.

15. Györke T. (2006) The role of imaging in psychiatric disorders: SPECT investigation. (Hungarian) Neuropsychopharmacol Hung, 8 Suppl.1: 58-63.

16. Horányi J, Szlávik R, Duffek L, Darvas K, Györke T, Lakatos P, Tóth M. (2006) Surgery of primary hyperparathyroidism. (Hungarian) Orv Hetil, 147: 2347-2351.

17. Kovács T, Farsang M, Vitaszil E, Barsi P, Györke T, Szirmai I, Kamondi A. (2009) Levetiracetam reduces myoclonus in corticobasal degeneration: report of two cases. J Neural Transm, 116: 1631-1634.
    IF: 2.259